HHS Public Access

Author manuscript

J Chem Neuroanat. Author manuscript; available in PMC 2017 October 01.

Published in final edited form as:

J Chem Neuroanat. 2016 October ; 76(Pt B): 108–121. doi:10.1016/j.jchemneu.2015.10.008.

Reduced GABA neuron density in auditory cerebral cortex of subjects with major depressive disorder

John F. Smiley[a,b,*], **Troy A. Hackett**[c], **Cynthia Bleiwas**[a], **Eva Petkova**[a,b], **Aleksandar Stankov**[g], **J. John Mann**[d,e], **Gorazd Rosoklija**[d,e,f], and **Andrew J. Dwork**[d,e,f]

[a]Program in Cognitive Neuroscience and Schizophrenia, Nathan Kline Institute for Psychiatric Research, Orangeburg, NY, USA

[b]Department of Child and Adolescent Psychiatry, New York University Langone Medical Center, New York, NY, USA

[c]Department of Psychology, Vanderbilt University School of Medicine, Nashville, TN, USA

[d]Division of Molecular Imaging and Neuropathology, New York State Psychiatric Institute and Columbia University, New York, NY, USA

[e]Department of Neuroscience, New York State Psychiatric Institute, New York, NY, USA

[f]Macedonian Academy of Sciences and Arts, Skopje, Macedonia

[g]Institute for Forensic Medicine, School of Medicine, Skopje, Macedonia

Abstract

Although disrupted function of frontal and limbic areas of cerebral cortex are closely associated with major depressive disorder (MDD) and schizophrenia (SZ), cellular pathology has also been found in other brain areas, including primary sensory areas. Auditory cortex is of particular interest, given the prominence of auditory hallucinations in SZ, and sensory deficits in MDD. We used stereological sampling methods in auditory cortex to look for cellular differences between MDD and SZ compared to non-psychiatric subjects. Additionally, as all of our MDD subjects died of suicide, we evaluated the association of suicide with our measurements by selecting a SZ sample that was divided between suicide and non-suicide subjects. Measurements were done in primary auditory cortex (area A1) and auditory association cortex (area Tpt), two areas with distinct roles in sensory processing and obvious differences in neuron density and size. In MDD, densities of GABAergic interneurons immunolabeled for calretinin (CR) and calbindin (CB) were 23–29% lower than non-psychiatric controls in both areas. Parvalbumin (PV) interneurons (counted only in area Tpt) showed a nominally smaller (16%) reduction that was not statistically significant. Total neuron and glia densities measured in Nissl stained sections did not show corresponding reductions. Analysis of suicide in the SZ sample indicated that reduced CR cell

Corresponding author: John F. Smiley, Ph.D., Program in Cognitive Neuroscience and Schizophrenia, Nathan Kline Institute for Psychiatric Research, 140 Old Orangeburg Rd., Orangeburg, NY 10962, Phone: 845-398-6601, Fax: 845-398-5531, smiley@nki.rfmh.org.

density was associated with suicide, whereas the densities of CB and other cells were not. Our results are consistent with previous studies in MDD that found altered GABA-associated markers throughout the cerebral cortex including primary sensory areas.

Keywords

interneuron; stereology; sensory cortex; human postmortem; psychiatric; schizophrenia; major depression; suicide

1. Introduction

MDD is defined by the presence of disrupted emotional processing, so investigations of brain pathology in MDD have generally focused on limbic and prefrontal regions that are central to emotional regulation. However, MDD is also associated with other cognitive deficits including sensory processing (Li et al., 2010; Schwenzer et al., 2012; Takei et al., 2009; Tollkotter et al., 2006; Zwanzger et al., 2012), and at least some cellular and molecular changes are found throughout the brain, even in disparate areas such as cerebellum and primary visual cortex (Fatemi et al., 2013; Li et al., 2013; Maciag et al., 2010; Sanacora et al., 2004). Among the most common findings are reduced glia- and GABA-associated markers, reduced markers for neurotrophic support and increased inflammatory markers (Aston et al., 2005; Choudary et al., 2005; Duric et al., 2010; Evans et al., 2004; Guilloux et al., 2012; Sequeira et al., 2007; Sequeira et al., 2012; Shelton et al., 2011; Tripp et al., 2012). However, it remains unclear how these changes are related to the onset and progression of MDD, or whether there is irreversible neuron loss.

One of the most consistent findings from postmortem MDD brains is the reduction of glial density or number in medial, oribital and dorsolateral prefrontal cortex (reviewed in (Hercher et al., 2009b; Rajkowska and Stockmeier, 2013)), although this was not found in all studies (Cotter et al., 2005; Hercher et al., 2009a). Reduction of neuronal density or number was not significant in most studies, but was recently reported in orbital and dorsolateral prefrontal cortex from depressed suicide subjects (Underwood et al., 2012), and in geriatric depression (Rajkowska et al., 2005). There are also reports of reduced numerical density of immunolabeled GABA neurons in both prefrontal and primary visual cortex, although it is unclear if this reflects reduced numbers of interneurons or alternatively reduced staining for GABAergic markers (Maciag et al., 2010; Rajkowska et al., 2007). The reduction was found in the calbindin (CB) but not parvalbumin (PV) interneuron subtypes, suggesting that MDD may be associated with a characteristic profile of altered GABAergic neurocircuitry. Subsequent mRNA expression studies of MDD also found reduced GABA-associated transcripts, especially for somatostatin that is highly colocalized with CB in interneurons (Guilloux et al., 2012; Sibille et al., 2011; Tripp et al., 2012). These findings in MDD are consistent with reports of altered expression of different GABA receptor mRNAs (Sequeira et al., 2009), and low GABA concentrations found by proton magnetic resonance spectroscopy of cerebral cortex or in CSF or serum [reviewed in(Mann et al., 2014; Sanacora and Saricicek, 2007)]. In vivo structural imaging of MDD brains has inconsistently shown

modestly reduced volume in prefrontal cortex, hippocampus and amygdala (Koolschijn et al., 2009; Lorenzetti et al., 2009).

Comparatively few studies have evaluated auditory regions in MDD. *In vivo* imaging did not show reduced cortical volume (Caetano et al., 2004; Morys et al., 2003), although reduced gray matter density was correlated with illness severity (Shah et al., 2002). Postmortem measurements in a brain sample from the Stanley Medical Research Institute did not detect altered densities of glia or neurons (Beasley et al., 2005; Cotter et al., 2004) even though reduced glial density was prominent in prefrontal cortex from the same brains (Cotter et al., 2002b).

SZ is associated with altered sensory processing (Javitt, 2009; Torrey, 2007), and auditory regions of the superior temporal gyrus have been especially implicated by *in vivo* imaging (Narr et al., 2005; Shenton et al., 2001). Auditory hallucinations are a prominent feature of SZ, however, our previous studies of auditory cortex in SZ compared area A1 with association cortex of the planum temporale, and found only subtle thinning of the left planum temporale, with unchanged neuron density and size (Smiley et al., 2013; Smiley et al., 2009; Smiley et al., 2011). In this and other regions of the cerebral cortex, findings of altered cellular organization in SZ cortex have been inconsistent [reviewed in (Dwork et al., 2009)]. There are some reports of fewer glia [e.g., (Rajkowska et al., 2002; Stark et al., 2004; Uranova et al., 2004)] increased neuron density [e.g., (Dorph-Petersen et al., 2009; Selemon et al., 2003)], and reduced neuron size (Pierri et al., 2003; Sweet et al., 2004). A more consistent finding is the down-regulation of GABA-related mRNAs and proteins, which is pronounced in about half of SZ subjects, found across diverse areas of cerebral cortex, and relatively selective for mRNA's associated with PV and CB, but not calretinin (CR) cells (Hashimoto et al., 2008; Hashimoto et al., 2003; Volk et al., 2012). While some studies found reduced overall density or number of GABA neurons (Beasley et al., 2002; Chance et al., 2005; Cotter et al., 2002a; Konradi et al., 2011; Reynolds et al., 2001; Wang et al., 2011; Zhang and Reynolds, 2002) others did not (Pantazopoulos et al., 2007; Woo et al., 1997). mRNA expression studies provided evidence that lower GABA-cell counts might reflect reduced expression of GABA cell markers, rather than cell loss (Hashimoto et al., 2003).

The present study revisits the issues of cell density and size in MDD and SZ compared to non-psychiatric subjects, evaluating both total neurons, identified with Nissl staining, and subtypes of immunolabeled GABA cells, in a brain sample that is independent from our previous studies in auditory cortex. Direct comparisons are made between A1 and Tpt, two cortical areas with very distinct profiles of cell density and size, and distinct roles in sensory processing. As before, we found little evidence for detectable cytoarchitectonic disruptions in SZ. However, in MDD subjects we found reduced density of immunolabeled GABAergic neurons.

2. Methods and Materials

2.1 Subjects

Brains were from the Institute for Forensic Medicine in Skopje Macedonia, and were selected to match diagnostic groups for gender, age, postmortem interval and storage time (Table 1). DSM-IV clinical diagnoses were established by psychological autopsy interview (Kelly and Mann, 1996). Brains were excluded if they met Khachaturian criteria for Alzheimer pathology or had clinical or pathological diagnoses of neurological disease. Brains were also excluded if there was a history of abuse or dependence associated with any substance except tobacco (Dwork et al., 1998). Additional review of the included cases did not reveal any cases with a history of head trauma or of emotional trauma including death of a parent or abuse during childhood. The study procedures were approved by the Institutional Review Boards of the New York State Psychiatric Institute, the Nathan Kline Institute, and the School of Medicine, University “Ss. Cyril & Methodius.”

Final included cortical samples were taken from 20 non-psychiatric, 17 MDD, and 14 SZ subjects. Three additional subjects (2 SZ and 1 non-psychiatric) were omitted due to poor immunolabeling with all antibodies. Some diagnostic comparisons used fewer samples (Table 2) because A1 or Tpt was damaged or unavailable, or because immunolabeling did not penetrate the tissue sections adequately to allow stereological sampling.

2.2 Histological Processing

Brain left hemispheres were sliced at autopsy into 2 cm thick coronal slabs that were placed in custom-made cassettes and immersed in phosphate-buffered 10% formalin at room temperature for 5 days, before storage at 4C in 0.05 M phosphate buffered saline with 0.02% sodium azide. The region containing the planum temporale and at least the caudal half of Heschl’s gyrus was dissected from these slabs, and reconstructed by embedding in a protein matrix, so that the entire region could be sectioned as a single block (Smiley and Bleiwas, 2012). 80 μm-thick frozen sections were cut on a calibrated sliding microtome, with the plane of section perpendicular to the axis of Heschl’s gyrus. Digital images of the block face were used to record the appearance of each section, and to make 3-dimensional reconstructions of the tissue, so that the location of each section in the original tissue was easily identified (Fig. 1A). A random number generator was used to select a series of every 12^{th} section through the sample, which were mounted and dried overnight on glass slides, Nissl-stained with thionine, dehydrated through increasing concentrations of ethanol and coverslipped in Permount (Fischer Scientific). Adjacent series of sections were processed for immunocytochemistry using 1:5,000 rabbit anti-CR (cat. # 7697, Swant Antibodies, Switzerland), 1:3,000 mouse anti-CB (cat. # 300, Swant) or 1:5,000 mouse anti-PV(cat. # 235, Swant). Sections were first processed for antigen retrieval by 4 cycles of heating to near boiling, separated by 30 second intervals, in 10 mM citric acid, pH 6.0. They were then exposed at 4C to primary antibodies for 3 days in 1% normal serum, 0.03% Triton X-100 and phosphate buffer, pH 7.4. Using rinses in phosphate buffer between steps, they were then immersed overnight at 4C in biotinylated secondary antibodies, followed by several hours in streptavidin-biotin-peroxidase (Vector laboratories) at room temperature. Labeling was visualized by tailoring the reaction time in 0.25 % diaminobenzidine with 0.06 %

hydrogen peroxide to achieve optimal cell labeling and penetration of the label into the tissue sections. Sections were then mounted on slides, left to dry overnight, dehydrated through graded series of ethanol to xylenes, and coverslipped with Permount.

2.3 Cell specificity of antibody labels

To determine the cellular specificity of the CB, CR and PV immunolabels, we used double labeling fluorescence in vibratome sections from the surface of the superior temporal gyrus adjacent to the planum temporale. Each experiment combined a mouse and rabbit primary antibody, and to visualize CB with PV we replaced the mouse anti-PV with rabbit-anti-PV (cat. # PV27, Swant). One primary antibody was labeled by a secondary anti-mouse or rabbit antibody conjugated to Alexa Flour 488 (Invitrogen cat # A11001 and A11008), and colocalization with a second primary antibody was visualized with a biotinylated anti-mouse or -rabbit antibody subsequently linked to streptavidin-conjugated Alexa Flour 594 (Invitrogen cat # S11227). Background fluorescence was monitored with an ultraviolet filter set, and digital images that included all 3 color channels were sampled by the optical dissector method across the depth of cortex, as previously described (Smiley et al., 2015). These experiments showed that double labeling was rare in all combinations of non-homologous antibodies, with faint and often uncertain detection of the colocalized label in < 2% of the cells.

2.4 Identification of Cortical Areas

A1 occupied approximately the caudal-medial half of Heschl's gyrus. As previously described, the borders of A1 were identified by its high cell density in layers II–III, small neuron size, lack of large pyramidal cells in layers III and V, comparatively indistinct layer III/IV border, and pale and wide appearance of layer V (Smiley et al., 2013). In our previous study we found that the precise borders of A1are ambiguous in a significant fraction of human brains. Therefore, in the present study we did not attempt to use A1 volumes to estimate total cell numbers, but instead sampled neuron densities from the unambiguously identified more central part of A1, using every 2^{nd} or 3^{rd} 0.96 mm spaced section, so that 4–8 evenly spaced sections were sampled from each A1.

Area Tpt was identified as described by Sweet et al. (Sweet et al., 2005), and corresponds to area Tpt of Galburda (Galaburda and Sanides, 1980) and to the superior temporal area of Wallace (Wallace et al., 2002). This area is lateral to the two bands of highly columnar cortex that Sweet et al. called internal and external parabelt, and Wallace et al. called the posterior area and lateral area. Area Tpt is less columnar than these medial areas, with appearance similar to that of inferior parietal cortex, and is typically located on the lateral surface of the planum temporale, sometimes extending onto the surface of the superior temporal gryus. As the precise borders of this area are difficult to identify, neuron densities were sampled in 4–6 consecutive 0.96 mm spaced sections at the approximate center of this area.

2.5 Cell Densities

All cell measurements were done on coded images so the rater was blind to diagnosis. Cell densities were evaluated using the optical dissector method (West and Gundersen, 1990),

using ImageJ software (http://imagej.nih.gov/) to operate a motorized Nikon E600 microscope and attached Foculus FO 442 digital camera (Phase GmbH, Germany). A photomontage was made of each section, using a 2x objective, and its pixel coordinates aligned to the X-Y coordinates of the microscope stage. Regions of interest were outlined on the photomontage, and the corresponding tissue sampled with a systematically random placed grid of optical disector sites (Fig. 1).

For counts of Nissl-stained cells, Z-stacks of 12 digital images with 1μm spacing were obtained at each dissector site, using a 100x oil immersion objective, N.A. = 1.3. To count neurons, an optical disector counting box was drawn on each Z-stack with X and Y dimensions = 49 μm, and Z = 5 μm, with an upper guard zone extending 2–4 μm from the tissue surface. For glia, the X-Y dimensions were reduced so that the counting box volume was one third of that used for neurons. Cell nuclei were counted, and neurons were identified by the presence of well-stained cytoplasmic Nissl substance, a thinner nuclear membrane, and a visible nucleolus, whereas glia had poorly stained cytoplasm, thicker nuclear membranes and inhomogeneous chromatin. Cells were not counted if they had elongated or irregularly shaped nuclei typical of endothelial cells and pericytes. For every dissector site, the distances from the pial surface and white matter border were recorded, so that cell density and size measures could be separated on the basis of cortical depth, as previously described (Smiley et al., 2012). Cell density measurements were corrected for Z-axis section shrinkage from the original 80 μm to the final thickness on the slide, measured in triplicate within area A1 or Tpt on every sampled section. Nissl stained section thickness did not differ between diagnostic groups ($p = 0.87$, group x area ANOVA) or between areas ($p = 0.21$; average = 21.5 +/− 2.3 microns, mean +/− S.D. in A1, and 22.1 +/− 2.5 in Tpt). On average, 240 +/− 30 (mean +/− S.D.) optical disectors were used from each area A1 or Tpt, with 375 +/− 73 neurons and 201 +/− 35 glia counted in each area, and average coefficients of error (CE) (Dorph-Petersen et al., 2009) of 0.06 +/− 0.02 for neuron densities and 0.08 +/− 0.04 for glia densities.

For counts of immunolabeled GABA cells, Z-stacks of 8 digital images with 2 μm spacing were obtained at each disector site, using a 50x oil immersion objective, N.A. = 1.3. Labeled cell soma were counted using a counting box with X,Y and Z dimensions of 150, 110, and 4 μm respectively, using an upper guard zone of 2 μm and lower guard zone of at least 2 μm. Final section thickness did not differ between diagnostic groups ($p = 0.35$, group x area x label ANOVA) or between immunolabels ($p = 0.52$). However, there was a significant difference between areas ($p < 0.001$) with thicker tissue (i.e., less shrinkage) in A1 (14.1 +/− 1.7) than Tpt (12.3 +/− 1.6). On average, 224 +/− 46 (mean +/− S.D.) optical disectors were used from each area A1 or Tpt, with 218 +/− 80 neurons counted in each area, and average coefficients of error (CE) (Dorph-Petersen et al., 2009) in area A1 were 0.09 +/− 0.03 and 0.10 +/− 0.05 (mean +/− S.D.) for CR and CB, respectively. In Tpt, CEs were 0.10 +/− 0.05, 0.09 +/− 0.05 and 0.07 +/− 0.02 for CR, CB and PV, respectively.

2.6 Tissue penetration of immunolabels

In some samples, incomplete tissue penetration of immunolabels prevented consistent placement of our 8-micron deep counting probe, that included a 4-micron counting box, and

2 micron upper and lower guard zones. Incomplete penetration was often associated with the intense PV labeling of the neuropil in the middle layers of A1, and for this reason PV neurons were evaluated only in area Tpt. In all other samples, we reviewed this issue by re-imaging and re-counting samples that had fewer than 45% of their cells counted in the lower half of the optical dissector. Based on these reviews, 11 of the remaining 225 samples from areas A1 or Tpt were omitted due to incomplete antibody penetration (see Results for further descriptions). The final average percent of cells in the lower half of the disector was 49+/− 5% (mean +/− S.D., N = 214 areas sampled), and this was nearly identical for each of the different immunolabels, and for area A1 and Tpt. Diagnostic comparisons for each label in either A1 or Tpt did not reveal any group differences in depth of counted cells (p values > 0.45, univariate ANOVAs).

2.7 Neuron Size and Labeling Density

Cell soma size was measured by the nucleator method (Gundersen, 1988) on every second Nissl stained neuron, and on every immunolabeled neuron counted for neuron density. Glia cells were not measured, as cytoplasm was poorly visualized. The average cell radius was determined from 3 isotropic random lines extending from a point at the approximate center of the Nissl stained nucleus or the immunolabled cell soma, to the intersection with the cell membrane. Estimates of measurement precision (Dorph-Petersen et al., 2004) for Nissl stained neurons produced CEs of 0.03 +/− 0.01 in A1 and 0.05 +/− 0.01 in Tpt. For immunolabeled neurons CEs in A1 were 0.05 +/− 0.02 and 0.06 +/− 0.01, for CR and CB, respectively. In Tpt, CEs were 0.04 +/− 0.02, 0.6 +/− 0.01 and 0.04 +/− 0.01, for CR, CB and PV, respectively.

To evaluate cell immunolabeling density, we determined the difference between the mean gray-scale density measured at a 5 micron diameter circle at the center of each cell and the modal gray scale value outside the cell sampled in a circular band located at a radius of 55 to 60 microns from the cell center (Fig. 1D).

2.8 Cortical thickness

Cortical thickness was measured as previously described (Smiley et al., 2012; Smiley et al., 2009). Briefly, on every available Nissl-stained section through Heschl's gyrus and the planum temporale, outlines were made of the cortical surface, the layer III–IV border, and the white matter border. Shortest distances between these borders were displayed as colored flat-maps from which regional median thicknesses were obtained. Tangentially cut cortex, identified by upper or lower layers thicker than 1.95 mm, was omitted. Inclusion of these tangential sections did not significantly affect diagnostic group comparisons (data not shown). Besides total cortex thickness presented here, these analyses provided measurements of upper (I–III) and lower (IV–VI) layer thickness, and of the volume fractions of the upper and lower layers, as previously described (Smiley et al., 2012), which did not differ between diagnostic groups (data not shown).

Cortex thickness has local variations due to cortical folding. Therefore, measurements were taken from the larger regions of Heschl's gyrus and the planum temporale, in addition to local measurements at the of A1 and Tpt sites used for cell measurements. Thickness

measurements from the whole planum temporale included 27 +/−6 sections through Heschl's gyrus, and 26 +/− 5 sections (mean +/− S.D) through the planum temporale. The number of sections in either region did not differ between diagnostic groups (p values > 0.60). Separate evaluations of the rostral and caudal planum temporale each used half of the available sections.

2.9 Statistical Analyses

Estimating the effect of diagnosis on the all outcomes was based on linear models. Nine of the outcomes were measured at 2 areas of the brain, and their analyses were based on linear mixed effects models. The two outcomes per person (one for each area) were modeled as a function of diagnosis (3 levels), area (2 levels) and their interaction. The significance of the interaction terms was judged based on likelihood ratio test (Chi-square test on 2 d.f.). If the interaction term was significant (at level α=0.05 two-sided), the pairwise comparisons between diagnoses was made separately for each area. If the interaction term was not significant, the model was refit with only main effects for diagnosis and area. The significance of the diagnosis and area factors was judged based on that model. The potential correlation between the outcomes measured on the same subject (one from each brain area), was accounted for by the inclusion of random subject effects. The variances of the random subject effects were allowed to be different depending on a diagnostic group. Three of the outcomes (PV density, size and labeling density) were measured only in area Tpt, and the effect of diagnosis on those outcomes was based on linear regression models that had diagnosis as a predictor.

We also explored the effects of (i) suicide (yes/no), (ii) use of tricyclic medication (yes/no), (iii) use of SSRIs (yes/no) and (iv) duration of antipsychotic use on the inferences regarding differences between diagnoses with respect to all outcomes. This was accomplished by including in the main effect of the covariate and its interaction with diagnosis (and with area and area-by-diagnosis when the outcome is measured at two brain areas) to the models described above. A statistically significant interaction with diagnosis would indicate that the relationships between diagnoses depend on the level of the covariate and in such cases we estimated the differences between diagnoses at different levels of the covariate. If there were no significant interactions between the covariate and diagnosis, the main effect of the covariate was assessed from a model that omitted such interactions.

In all models we controlled for the effects of (a) age, (b) gender, (c) post-mortem interval and (d) brain storage time, by including main effects of these variables in all models regardless of their significance. We acknowledge that it would be appropriate to control also for (e) brain pH. However, brain pH was not assessed on 6 subjects, because frozen tissue was not available. For this reason, we consider the results from the analyses that control also for pH as secondary and report results from those analyses only when they differ from the main analyses described above.

All analyses were conducted adjusting for age, sex, pmi, and brain storage time. Raw p-values are reported without an adjustment for multiple testing. Results that are expressed as percent changes for diagnostic comparisons were calculated as = 100×(1− (MDD or SZ)/ non-psychiatric), or 100×(1−(MMD/SZ)). The analysis was conducted in R [R Core Team

(2013). R: A Language and Environment for Statistical Computing. R Foundation for Statistical Computing, Vienna, Austria. <URL: http://www.R-project.org/>] using the package “lme4” from CRAN <https://cran.r-project.org/>.

3. Results

3.1 Nissl stained neurons and glia

As expected from the qualitative criteria used to identify A1, it had higher neuron density and smaller size compared to Tpt. In contrast, the density of glial cells was similar in A1 and Tpt (Fig. 2, Table 2). Separation of measurements by depth of cortex indicated that the area differences in neuron density and size were present across cortical layers (Fig. 2).

Diagnostic comparisons of total neuron densities showed qualitative evidence for modestly lower neuron density in A1 of MDD subjects (9% less than in non-psychatric subjects). However, this difference was not present in area Tpt, and statistical analysis did not reveal a significant diagnostic difference ($p = 0.12$) or area x diagnosis interaction ($p= 0.16$). Similarly, the total glia cell density did not differ between groups ($p = 0.48$) or show an area x diagnosis interaction ($p = 0.78$; Fig. 3 and Table 2). Separation of these measurements by depth of cortex did not provide evidence for obvious group differences in individual cortical layers (Supplemental Fig. 1).

Evaluation of total neuron size showed a significant effect of diagnosis in the primary statistical model ($p < 0.02$), but this was not significant in the secondary model that also included pH as a covariate ($p = 0.14$, Table 2). Further investigation showed that the three diagnostic groups did not differ with respect to pH, but neuronal size correlated negatively with pH, across all diagnostic groups, in both area A1 ($r = -0.42$, $p < 0.05$) and Tpt ($r = -0.33$, $p < 0.05$). There was no evidence of a diagnosis x area interaction of cell size ($p = 0.90$). Separation of cell size measurements by depth of cortex showed that the slightly larger cell size in the MDD group was present across layers in both areas A1 and Tpt (Figure 4).

3.2 Parvalbumin neurons

PV cells were not analyzed in A1, due to poor penetration of the immunolabel in the intensely labeled middle layers. In Tpt, penetration of the PV label was usually excellent, but 5 cases (2 non-psychiatric, 2 MDD, and 1 SZ) were excluded due to inadequate penetration.

In area Tpt, PV neuron density was about 16% less in MDD subjects compared to non-psychiatric or SZ subjects, but the difference was not statistically significant ($p = 0.13$; Table 2, Fig. 5A). Plots of PV cell density by depth of cortex showed similar laminar distributions in the three diagnostic groups (Supplementary Fig. 2A). Measurements of PV neuron size and labeling density did not reveal diagnostic differences (Table 2).

3.3 Calbindin neurons

In CB labeled tissue, 5 samples were omitted due to inadequate penetration of the immunolabel (A1: 2 MDD and 2 non-psychiatric; Tpt: 1 non-psychiatric). In the remaining samples, density showed a significant diagnostic difference ($p < 0.0001$) but did not reveal a

diagnosis x area interaction ($p = 0.90$). Follow-up analysis showed that MDD cases had 23–24% lower densities than non-psychiatric cases in both areas A1 and Tpt. In SZ subjects, CB neuron densities were slightly but not significantly greater than those of non-psychiatric densities (Table 2, Fig. 5B). Plots by depth of cortex showed that CB cells were mainly concentrated in the upper cortical layers, and did not show evidence of laminar specificity of altered density in MDD (Supplementary Fig. 2B).

CB neuron size was significantly different between diagnostic groups ($p = 0.03$). As with measurement of total neurons, the CB cells were 5–6% larger in both A1 and Tpt of MDD subjects compared to non-psychiatric or SZ subjects. The labeling density of CB neurons did not differ between diagnostic groups (Table 2).

3.4 Calretinin neurons

Two CR samples were omitted due to poor immunolabel penetration, including area A1 and area Tpt from the same MDD brain. In the remaining brains, diagnostic comparisons of neuron densities showed a significant diagnostic difference ($p < 0.0001$) but did not show a diagnosis x area interaction ($p = 0.57$). Similar to CB cells, CR cell densities in MDD were 26–29% lower compared to non-psychiatric cases in areas A1 and Tpt, whereas SZ cell densities were similar to those of non-psychiatric subjects (Table 2, Fig. 5C). However, as described below, the SZ subjects that died by suicide had low CR densities similar to the MDD subjects, indicating that lower CR density in the MDD subjects could be associated with suicidal behavior.

Plots of cell densities by depth of cortex showed that CR cells were mainly concentrated in the upper cortical layers, and there was no obvious laminar specificity of altered density in MDD (Supplementary Fig. 2C).

In contrast to CB and PV cells, there was additionally evidence for group differences in CR cell labeling density. Because there was a significant diagnosis x area interaction ($p < 0.01$), the main diagnosis effect was evaluated separately for each area. In area Tpt, reduced label density in MDD subjects compared to non-psychiatric subjects was significant ($p<0.001$), but in A1 it showed only trend-level significance (0.06; Table 2).

3.5 Cortical thickness

Comparisons of cortex thickness in the regions of Heshcl’s gyrus and the planum temporale (ANOVA; diagnosis x region) did not show significant diagnostic differences ($p = 0.63$) or area x diagnosis interaction ($p < 0.47$). There was an effect of region ($p = 0.04$), due to thinner cortex in Heschl’s gyrus compared to the planum temporale. Further subdivision of the planum temporale into rostral and caudal parts, also did not reveal group differences, but showed thicker cortex in rostral compared to caudal planum temporale ($p = 0.02$). These regional differences were not observed previously (Smiley et al., 2009), and likely reflect the plane of section in the present study, which was optimized to provide perpendicular sections through Heschl’s gyrus. More localized thickness measurements, at the sites of A1 and Tpt sampled for neuron density, showed cortex thickness similar to that of the larger regions (Table 3).

3.6 Suicide and pharmacological treatments

Additional exploratory analyses were used to test possible effects of suicide and pharmacological treatments on our outcome measures. While all of our MDD subjects died by suicide, in the SZ group 8 of 14 subjects died of suicide. Analysis of the effect of suicide showed a significant main effect on CR cell density ($p = 0.001$): within the SZ subjects, CR density in suicide subjects was 22 and 30% lower in areas Tpt and A1 respectively, than in non-suicide subjects (Fig. 5C). In contrast, there was no evidence for an association of suicide with CB cell density ($p = 0.44$) or PV cell density ($p = 0.19$). Evaluation of other outcome measures showed that suicide was positively associated with increased CB labeling density only in area Tpt ($p < 0.01$).

Additional analyses showed that tricyclic antidepressant treatment (N = 8 of 17 MDD, and 4 of 14 SZ) was associated with increased CR cell density ($p = 0.012$). Evaluation of the small group of subjects who were treated with SSRIs, including 4 MDD subjects who also received tricyclic antidepressants and 1 SZ subject, showed evidence for a positive association with increased CB labeling density ($p < 0.01$) and with thicker cerebral cortex ($p< 0.01$). Finally, years of antipsychotic treatment (N= 14 SZ and 1 MDD) did not show a significant association with any outcome measure.

4. Discussion

4.1 Normal cell densities in human auditory cortex

To our knowledge, this is the first study using stereologically measured cell density and size to compare human primary auditory cortex directly with higher order association cortex. Our measurements confirm the well known features of higher neuron density and smaller neurons in A1 [e.g., (von Economo, 1929)], and show that these features are present in lower as well as upper cortical layers. Our finding also showed that glia densities, in contrast to neurons, were not significantly different between A1 and Tpt. One could have expected otherwise, considering that previous qualitative studies showed greater vascularization in A1 than in surrounding areas (Cobb, 1932). While we excluded cells with the appearance of vascular endothelial cells and pericytes, it might be expected that a higher density of blood vessel-associated astroglia would be present in A1. Future studies with more specific glial markers might reveal subtle differences between these areas. Overall, in our non-psychiatric brains, the ratio of glia to neurons was 1.8 in Tpt, and 1.5 in A1, similar to previously reported ratios of 1.4 in whole human neocortex (Pelvig et al., 2008) or 1.6–1.7 in prefrontal regions (Ongur et al., 1998; Rajkowska et al., 1999).

Our study also provides a stereological estimate of the relative abundance of PV, CB and CR neurons in human auditory cortex. In monkey prefrontal cortex, a stereological study concluded that these 3 neuron subsets accounted for about 22% of the total neuron population, including 11% CR neurons, 6% PV neurons, and 5% CB neurons (Gabbott and Bacon, 1996). Our estimates in area Tpt of non-psychiatric subjects were similar: CR neurons were 8% of the total population, PV neurons 5%, and CB neurons 6%, giving a total of 19%. The slightly lower estimate compared to monkey cortex could be due to technical limitations of human postmortem immunostaining, species differences or differences

between cortical regions (Clemo et al., 2003; Hendry et al., 1987). In A1, the proportion of CR and CB neurons in our non-psychiatric sample (7% and 5%, respectively) was slightly lower than in Tpt. In monkey cortex, it is estimated that about 25% of the total neuron population is GABAergic, indicating that our study surveyed as many as 80–90% of the cortical GABA cells by using these three antibodies to calcium binding proteins (Gabbott and Bacon, 1996; Hendry et al., 1987).

4.2 Cellular changes in MDD

CB and CR cell densities were 23–29% lower in our MDD sample, in both areas A1 and Tpt, whereas the statistically non-significant reduction in PV cells was about 16%. These findings are similar to a previous study by Rajkowska et al. [(Rajkowska et al., 2007)] who found reduced CB but not PV cells, in prefrontal areas 9 and 47, and subsequently replicated the CB deficit in primary visual cortex (Maciag et al., 2010). In contrast, CB, CR or PV cell densities were not altered in prefrontal areas 9 and 32 in a series of brains from the Stanley Medical Research Institute (Beasley et al., 2002; Cotter et al., 2002a). It is possible that we encountered comparatively large deficits because our MDD subjects were severely ill, with 12 of 17 subjects suffering from severe and/or recurrent depression, and all committing suicide. Our results are consistent with analyses of CSF and *in vivo* proton magnetic resonance spectroscopy that found larger GABA deficits in more severely depressed subjects (Roy et al., 1991; Sanacora et al., 2004).

In our comparison of SZ subjects with and without suicide, we did not find evidence that CB cell density is associated with suicide, and this is consistent with a previous study that showed MDD subjects with or without suicide had similar reductions of CB cell density (Maciag et al., 2010). Similarly, altered expressions of several GABA-receptor mRNAs in MDD were not present in a matched group of suicide subjects without depression (Sequeira et al., 2009). However, we did find an association of CR cell density with suicide in our SZ sample. While these findings need to be replicated in a larger sample, it suggests that CB and CR cells may be differentially involved in the pathological mechanisms associated with depression and suicide. It has been proposed that suicidal behavior may involve characteristic biological processes, including altered stress responses especially involving the hypothalamic-pituitary axis and monoamine systems (Oquendo et al., 2014). Consistent with the idea that reduced GABA may be associated with suicidal behavior, a large study of MDD subjects showed an inverse correlation between CSF GABA concentrations and anxiety (Mann et al., 2014).

Selective down-regulation in subtypes of cortical interneurons in MDD was also indicated by mRNA expression studies in prefrontal area 9, subgenual cingulate cortex, and amygdala (Guilloux et al., 2012; Sibille et al., 2011; Tripp et al., 2012). Each of these areas had decreased somatostatin, which is predominantly expressed by CB cells (DeFelipe, 1997), but reductions of PV and CR transcripts were less consistently found. From these findings it was hypothesized that GABA changes in MDD may be somewhat distinct from those of SZ, in which reduced expression of PV and CB/somatostatin but not CR transcripts, has been more commonly described (Sibille et al., 2011).

Our findings showed very similar GABA cell reductions in primary sensory cortex and association cortex in MDD. While we have not examined prefrontal cortex, our findings are consistent with previous demonstrations of comparable GABA reductions in prefrontal association and occipital visual sensory areas (Bhagwagar et al., 2008; Maciag et al., 2010). In this respect, altered GABA expression might be distinct from glial changes in MDD, which were not found in the present or previous studies of sensory cortex. Specifically, direct comparisons showed lower glia number in the subgenual cingulate cortex but not in somatosensory cortex of the postcentral gyrus (Ongur et al., 1998). Similarly, in a Stanley Institute brain sample, lower glial density was found in prefrontal area 9, but not in auditory cortex (Beasley et al., 2005; Beasley et al., 2009; Cotter et al., 2002b).

As with most studies of GABA neuron cell counts, we cannot definitively distinguish cell loss from reduced expression of GABA immunolabels. Precedent for the latter scenario was encountered in a mouse model of perinatal hypoxia, that caused reduced PV and somatostatin cell counts that persisted to adulthood, but could be normalized by exposing animals to an enriched environment, apparently due to upregulation of the immunoreactive PV and somatostatin without neurogenesis of new interneurons (Komitova et al., 2013). Dynamic levels of GABA expression have also been demonstrated in MDD subjects, where GABA detected by magnetic resonance spectroscopy was up-regulated by SSRIs (Bhagwagar et al., 2004; Sanacora et al., 2002). Similarly, in rodents, both stress and corticosteroids have been shown to reduce GABA and to alter expression of GABA receptors, and these effects were normalized by antidepressant medications in at least some models (Maguire, 2014; Sanacora and Saricicek, 2007; Skilbeck et al., 2010). Consistent with these findings, our exploratory analyses of the effects of pharmacological interventions showed higher CR cell density and CB cell labeling density in subjects with different antidepressant treatments. Alternatively, we cannot rule out the possibility that GABA cell number is truly reduced in our MDD subjects, either as consequence of disease associated neurotoxicity, or as a pre-existing condition that contributes to the vulnerability to MDD.

Measurements of total neuron density showed a statistically non-significant 9% reduction in A1 of MDD compared to non-psychiatric subjects, that was not found in areas Tpt, nor in estimates of total glia cell density. In a preliminary presentation of this finding, we reported a larger reduction of neuron density in A1 of MDD subjects (Smiley et al., 2014). However, review of those preliminary measurements showed high coefficients of error due to under-sampling of some brains, and for the current study all brains were re-imaged and re-counted with high sampling densities. Reduced total neuron density could partially be explained by loss of GABA neurons: for example an overall decrease of 20% of GABA neurons would predict roughly 5% loss of the total neurons. Arguing against this interpretation is the absence of a similar reduction of total neuron density in Tpt, where GABA cell reductions were similar to A1.

We additionally found a marginally significant increase of neuron size in our MDD brains. This was unlikely to be caused simply by loss of small GABAergic neurons, because it was also present in lower cortical layers that have proportionally few GABA cells, and a similar increase in cell size was present in CB neurons. In contrast, reduced neuron size has been reported in prefrontal cortex and hippocampus in a series of brains from Rajkowska and

colleagues (Rajkowska et al., 1999; Rajkowska et al., 2007; Stockmeier et al., 2004), and in brains from the Stanley Institute (Chana et al., 2003; Cotter et al., 2002b; Cotter et al., 2001). However, the latter brain sample did not have reduced neuron size in auditory cortex (Beasley, 2005). Another small study of MDD cingulate cortex found increased neuron size in MDD (Gittins and Harrison, 2011).

4.3 Cellular changes in SZ

We did not find altered GABA cell densities in SZ cortex, even though the most commonly reported finding with respect to CB, CR and PV cell densities is that CB and/or PV cells are decreased, but CR cells are not. Nearly 40% lower PV density, but not CR density, was reported in prefrontal cortex by Reynolds et al. (2001). Subsequent studies in an independent brain sample from the Stanley Medical Research Institute showed about 10%–50% deficits of PV and/or CB cells in prefrontal, cingulate, and hippocampal areas, whereas CR cell densities again were unaltered (Beasley et al., 2002; Cotter et al., 2002a; Zhang and Reynolds, 2002). Yet another brain sample had reduced CB cells in auditory cortex (Chance et al., 2005). More recently, measurements in the hippocampus and entorhinal cortex again showed evidence of striking reductions of PV and somatostatin interneurons (Konradi et al., 2011; Wang et al., 2011). The literature is not completely consistent, however, as two reasonably powered postmortem samples found unchanged PV cell density in prefrontal and entorhinal cortex (Pantazopoulos et al., 2007; Woo et al., 1997). In the context of this literature, we had expected to see at least some evidence of reduced CB or PV cells in our samples of auditory cortex.

Our finding of unchanged total neuron density and size in SZ cortex is consistent with our previous neuron measurements from separate brain samples in auditory cortex and nearby parietal cortex (Smiley et al., 2012; Smiley et al., 2011), and in auditory areas in a brain sample from the Stanley Medical Research Institute (Beasley et al., 2005; Cotter et al., 2004). Somewhat different results were obtained in another brain sample, that had reduced neuron size especially in layer III across auditory areas, and increased density of pyramidal shaped neurons in layer III of area A1 (Dorph-Petersen et al., 2009; Sweet et al., 2004). In general, these collected findings from auditory cortex are similar to results from other cortical areas, that usually but not always failed to show significant differences in neuron density and size in SZ [reviewed in (Dwork et al., 2009; Smiley et al., 2011), and see (Konradi et al., 2011)]. Perhaps a parsimonious synthesis of these findings is that small changes in SZ are typically beneath the sensitivity of detection for most postmortem sample sizes. For example, estimates of cortical thickness usually find reductions of about < 5% in SZ [e.g., (Goldman et al., 2009)]. Assuming that thinner cortex corresponds directly to changes in neuron density, this predicts that neuron density should be increased <5%. In the present study, we found non-significant neuron density increases of about 5% (3% in A1 and 8% in Tpt). Using the percent coefficient of variation of 14% from these measurements, a power analysis predicts that sample sizes > 100 subjects per group are needed to achieve statistical power of 0.8 to detect this difference (Faul et al., 2007).

We previously reported subtle cortical thinning in the caudal planum temporale, that was found mainly in the upper cortical layers of the caudal portion of the planum temporale

(Smiley et al., 2009). This was not found in the present study, perhaps due to the difficulty of detecting this small effect, or possibly due to technical differences between preparations. In particular, the current sample was sectioned perpendicular to the plane of Heschl's gyrus instead of coronally, thus displaying the planum temporale in a more tangentially cut plane of section.

4.4 Conclusions

Comparisons of two cortical areas that represent distinct stages of cortical sensory processing showed that both have comparable reductions of GABA interneurons in MDD. This is consistent with previous findings across diverse regions of MDD cerebral cortex that showed reduced GABA cells, reduced GABA concentrations, and altered mRNAs for GABA receptors and other GABA-associated markers. Consistent with previous studies in MDD sensory cortex, we did not find group differences in glial density, and it is possible that the reduction of glial cells may be restricted to prefrontal and limbic cortical regions, in contrast to the reduced density of GABA cells. Comparison of different interneuron subtypes in our sample indicated that the diagnostic differences in CB and CR cells were most pronounced, whereas the smaller differences in PV cells were not statistically significant. Evidence for lower CR cell density was additionally found in SZ-suicide subjects, suggesting that lower CR cell density in MDD may be to some extent associated with suicidal behavior. This profile of cell specific differences in MDD is in approximate agreement with previous cell counting and mRNA expression studies, that more consistently found altered expression associated with CB cells, and less consistently with PV and CR cells. In our SZ sample, we did not detect evidence of similar GABA cell reductions, even though that is the more common finding in other cortical regions.

Supplementary Material

Refer to Web version on PubMed Central for supplementary material.

Acknowledgments

This research was supported by NIMH grants MH085208, MH086385 MH64168, MH60877, MH87986, and the American Foundation for Suicide Prevention.

References

Aston C, Jiang L, Sokolov BP. Transcriptional profiling reveals evidence for signaling and oligodendroglial abnormalities in the temporal cortex from patients with major depressive disorder. Mol Psychiatry. 2005; 10:309–322. [PubMed: 15303102]

Beasley CL, Chana G, Honavar M, Landau S, Everall IP, Cotter D. Evidence for altered neuronal organisation within the planum temporale in major psychiatric disorders. Schizophr Res. 2005; 73:69–78. [PubMed: 15567079]

Beasley CL, Honavar M, Everall IP, Cotter D. Two-dimensional assessment of cytoarchitecture in the superior temporal white matter in schizophrenia, major depressive disorder and bipolar disorder. Schizophr Res. 2009; 115:156–162. [PubMed: 19833481]

Beasley CL, Zhang ZJ, Patten I, Reynolds GP. Selective deficits in prefrontal cortical GABAergic neurons in schizophrenia defined by the presence of calcium-binding proteins. Biol Psych. 2002; 52:708–715.

Bhagwagar Z, Wylezinska M, Jezzard P, Evans J, Boorman E, PMM, PJC. Low GABA concentrations in occipital cortex and anterior cingulate cortex in medication-free, recovered depressed patients. Int J Neuropsychopharmacol. 2008; 11:255–260. [PubMed: 17625025]

Bhagwagar Z, Wylezinska M, Taylor M, Jezzard P, Matthews PM, Cowen PJ. Increased brain GABA concentrations following acute administration of a selective serotonin reuptake inhibitor. Am J Psychiatry. 2004; 161:368–370. [PubMed: 14754790]

Caetano SC, Hatch JP, Brambilla P, Sassi RB, Nicoletti M, Mallinger AG, Frank E, Kupfer DJ, Keshavan MS, Soares JC. Anatomical MRI study of hippocampus and amygdala in patients with current and remitted major depression. Psychiatry Res. 2004; 132:141–147. [PubMed: 15598548]

Chana G, Landau S, Beasley C, Everall IP, Cotter D. Two-dimensional assessment of cytoarchitecture in the anterior cingulate cortex in major depressive disorder, bipolar disorder, and schizophrenia: evidence for decreased neuronal somal size and increased neuronal density. Biol Psychiatry. 2003; 53:1086–1098. [PubMed: 12814860]

Chance SA, Walker M, Crow TJ. Reduced density of calbindin-immunoreactive interneurons in the planum temporale in schizophrenia. Brain Res. 2005; 1046:32–37. [PubMed: 15927548]

Choudary PV, Molnar M, Evans SJ, Tomita H, Li JZ, Vawter MP, Myers RM, Bunney WE Jr, Akil H, Watson SJ, Jones EG. Altered cortical glutamatergic and GABAergic signal transmission with glial involvement in depression. Proc Natl Acad Sci U S A. 2005; 102:15653–15658. [PubMed: 16230605]

Clemo HR, Keniston L, Meredith MA. A comparison of the distribution of GABA-ergic neurons in cortices representing different sensory modalities. J Chem Neuroanat. 2003; 26:51–63. [PubMed: 12954530]

Cobb, S. The cerebrospinal blood vessels. In: Penfield, W., editor. Cytology and cellular pathology of the nervous system. Paul B. Hoeber, Inc; New York: 1932. p. 575-610.

Cotter D, Hudson L, Landau S. Evidence for orbitofrontal pathology in bipolar disorder and major depression, but not in schizophrenia. Bipolar Disord. 2005; 7:358–369. [PubMed: 16026489]

Cotter D, Landau S, Beasley C, Stevenson R, Chana G, MacMillan L, Everall I. The density and spatial distribution of GABAergic neurons, labelled using calcium binding proteins, in the anterior cingulate cortex in major depressive disorder, bipolar disorder, and schizophrenia. Biol Psychiatry. 2002a; 51:377–386. [PubMed: 11904132]

Cotter D, Mackay D, Chana G, Beasley C, Landau S, Everall IP. Reduced neuronal size and glial cell density in area 9 of the dorsolateral prefrontal cortex in subjects with major depressive disorder. Cereb Cortex. 2002b; 12:386–394. [PubMed: 11884354]

Cotter D, Mackay D, Frangou S, Hudson L, Landau S. Cell density and cortical thickness in Heschl's gyrus in schizophrenia, major depression and bipolar disorder. Br J Psychiatry. 2004; 185:258–259. [PubMed: 15339832]

Cotter D, Mackay D, Landau S, Kerwin R, Everall I. Reduced glial cell density and neuronal size in the anterior cingulate cortex in major depressive disorder. Arch Gen Psych. 2001; 58:545–553.

DeFelipe J. Types of neurons, synaptic connections and chemical characteristics of cells immunoreactive for calbindin-D28K, parvalbumin and calretinin in the neocortex. J Chem Neuroanat. 1997; 14:1–19. [PubMed: 9498163]

Dorph-Petersen KA, Delevich KM, Marcsisin MJ, Zhang W, Sampson AR, Gundersen HJ, Lewis DA, Sweet RA. Pyramidal neuron number in layer 3 of primary auditory cortex of subjects with schizophrenia. Brain Res. 2009; 1285:42–57. [PubMed: 19524554]

Dorph-Petersen KA, Pierri JN, Sun Z, Sampson AR, Lewis DA. Stereological analysis of the mediodorsal thalamic nucleus in schizophrenia: volume, neuron number, and cell types. J Comp Neurol. 2004; 472:449–462. [PubMed: 15065119]

Duric V, Banasr M, Licznerski P, Schmidt HD, Stockmeier CA, Simen AA, Newton SS, Duman RS. A negative regulator of MAP kinase causes depressive behavior. Nat Med. 2010; 16:1328–1332. [PubMed: 20953200]

Dwork A, Liu D, Kaufman M, Prohovnik I. Archival, formalin-fixed tissue: its use in the study of Alzheimer's type changes. Clin Neuropathol. 1998; 17:45–49. [PubMed: 9496540]

Dwork, AJ.; Smiley, JF.; Colibazzi, T.; Hoptman, MJ. Postmortem and *in vivo* structural pathology in schizophrenia. In: Charney, DS.; Nestler, EJ., editors. Neurobiology of Mental Illness. Oxford University Press; Oxford: 2009. p. 281-302.

Evans SJ, Choudary PV, Neal CR, Li JZ, Vawter MP, Tomita H, Lopez JF, Thompson RC, Meng F, Stead JD, Walsh DM, Myers RM, Bunney WE, Watson SJ, Jones EG, Akil H. Dysregulation of the fibroblast growth factor system in major depression. Proc Natl Acad Sci U S A. 2004; 101:15506–15511. [PubMed: 15483108]

Fatemi SH, Folsom TD, Rooney RJ, Thuras PD. Expression of GABAA alpha2-, beta1- and varepsilon-receptors are altered significantly in the lateral cerebellum of subjects with schizophrenia, major depression and bipolar disorder. Translational psychiatry. 2013; 3:e303. [PubMed: 24022508]

Faul F, Erdfelder E, Lang AG, Buchner A. G*Power 3: a flexible statistical power analysis program for the social, behavioral, and biomedical sciences. Behavioral Research Methods. 2007; 39:175–191.

Gabbott PL, Bacon SJ. Local circuit neurons in the medial prefrontal cortex (areas 24a,b,c, 25 and 32) in the monkey: II. Quantitative areal and laminar distributions. J Comp Neurol. 1996; 364:609–636. [PubMed: 8821450]

Galaburda A, Sanides F. Cytoarchitectonic organization of the human auditory cortex. J Comp Neurol. 1980; 190:597–610. [PubMed: 6771305]

Gittins RA, Harrison PJ. A morphometric study of glia and neurons in the anterior cingulate cortex in mood disorder. J Affect Disord. 2011; 133:328–332. [PubMed: 21497910]

Goldman AL, Pezawas L, Mattay VS, Fischl B, Verchinski BA, Chen Q, Weinberger DR, Meyer-Lindenberg A. Widespread reductions of cortical thickness in schizophrenia and spectrum disorders and evidence of heritability. Arch Gen Psych. 2009; 66:467–477.

Guilloux JP, Douillard-Guilloux G, Kota R, Wang X, Gardier AM, Martinowich K, Tseng GC, Lewis DA, Sibille E. Molecular evidence for BDNF- and GABA-related dysfunctions in the amygdala of female subjects with major depression. Mol Psychiatry. 2012; 17:1130–1142. [PubMed: 21912391]

Gundersen HJ. The nucleator. J Microsc. 1988; 151:3–21. [PubMed: 3193456]

Hashimoto T, Bazmi HH, Mirnics K, Wu Q, Sampson AR, Lewis DA. Conserved regional patterns of GABA-related transcript expression in the neocortex of subjects with schizophrenia. Am J Psychiatry. 2008; 165:479–489. [PubMed: 18281411]

Hashimoto T, Volk DW, Eggan SM, Mirnics K, Pierri JN, Sun Z, Sampson AR, Lewis DA. Gene expression deficits in a subclass of GABA neurons in the prefrontal cortex of subjects with schizophrenia. J Neurosci. 2003; 23:6315–6326. [PubMed: 12867516]

Hendry SHC, Schwark HD, Jones EG, Yan J. Numbers and proportions of GABA-immunoreactive neuron in different areas of monkey cerebral cortex. J Neurosci. 1987; 7:1503–1519. [PubMed: 3033170]

Hercher C, Parent M, Flores C, Canetti L, Turecki G, Mechawar N. Alcohol dependence-related increase of glial cell density in the anterior cingulate cortex of suicide completers. J Psychiatry Neurosci. 2009a; 34:281–288. [PubMed: 19568479]

Hercher C, Turecki G, Mechawar N. Through the looking glass: examining neuroanatomical evidence for cellular alterations in major depression. J Psychiatr Res. 2009b; 43:947–961. [PubMed: 19233384]

Javitt DC. When doors of perception close: bottom-up models of disrupted cognition in schizophrenia. Annu Rev Clin Psychol. 2009; 5:249–275. [PubMed: 19327031]

Kelly TM, Mann JJ. Validity of DSM-III-R diagnosis by psychological autopsy: a comparison with clinician ante-mortem diagnosis. Acta Psychiatr Scand. 1996; 94:337–343. [PubMed: 9124080]

Komitova M, Xenos D, Salmaso N, Tran KM, Brand T, Schwartz ML, Ment L, Vaccarino FM. Hypoxia-induced developmental delays of inhibitory interneurons are reversed by environmental enrichment in the postnatal mouse forebrain. J Neurosci. 2013; 33:13375–13387. [PubMed: 23946395]

Konradi C, Yang CK, Zimmerman EI, Lohmann KM, Gresch P, Pantazopoulos H, Berretta S, Heckers S. Hippocampal interneurons are abnormal in schizophrenia. Schizophr Res. 2011; 131:165–173. [PubMed: 21745723]

Koolschijn PC, van Haren NE, Lensvelt-Mulders GJ, Hulshoff Pol HE, Kahn RS. Brain volume abnormalities in major depressive disorder: a meta-analysis of magnetic resonance imaging studies. Hum Brain Mapp. 2009; 30:3719–3735. [PubMed: 19441021]

Li CT, Lin CP, Chou KH, Chen IY, Hsieh JC, Wu CL, Lin WC, Su TP. Structural and cognitive deficits in remitting and non-remitting recurrent depression: a voxel-based morphometric study. Neuroimage. 2010; 50:347–356. [PubMed: 19931620]

Li JZ, Bunney BG, Meng F, Hagenauer MH, Walsh DM, Vawter MP, Evans SJ, Choudary PV, Cartagena P, Barchas JD, Schatzberg AF, Jones EG, Myers RM, Watson SJ Jr, Akil H, Bunney WE. Circadian patterns of gene expression in the human brain and disruption in major depressive disorder. Proc Natl Acad Sci U S A. 2013; 110:9950–9955. [PubMed: 23671070]

Lorenzetti V, Allen NB, Fornito A, Yucel M. Structural brain abnormalities in major depressive disorder: a selective review of recent MRI studies. J Affect Disord. 2009; 117:1–17. [PubMed: 19237202]

Maciag D, Hughes J, O'Dwyer G, Pride Y, Stockmeier CA, Sanacora G, Rajkowska G. Reduced density of calbindin immunoreactive GABAergic neurons in the occipital cortex in major depression: relevance to neuroimaging studies. Biol Psychiatry. 2010; 67:465–470. [PubMed: 20004363]

Maguire J. Stress-induced plasticity of GABAergic inhibition. Front Cell Neurosci. 2014; 8:157. [PubMed: 24936173]

Mann JJ, Oquendo MA, Watson KT, Boldrini M, Malone KM, Ellis SP, Sullivan G, Cooper TB, Xie S, Currier D. Anxiety in major depression and cerebrospinal fluid free gamma-aminobutyric acid. Depress Anxiety. 2014; 31:814–821. [PubMed: 24865448]

Morys JM, Bobek-Billewicz B, Dziewiatkowski J, Ratajczak I, Pankiewicz P, Narkiewicz O, Morys J. A magnetic resonance volumetric study of the temporal lobe structures in depression. Folia Morphol (Warsz). 2003; 62:347–352. [PubMed: 14655115]

Narr KL, Bilder RM, Toga AW, Woods RP, Rex DE, Szeszko PR, Robinson D, Sevy S, Gunduz-Bruce H, Wang YP, DeLuca H, Thompson PM. Mapping cortical thickness and gray matter concentration in first episode schizophrenia. Cereb Cortex. 2005; 15:708–719. [PubMed: 15371291]

Ongur D, Drevets WC, Price JL. Glial reduction in the subgenual prefrontal cortex in mood disorders. Proc Natl Acad Sci. 1998; 95:13290–13295. [PubMed: 9789081]

Oquendo MA, Sullivan GM, Sudol K, Baca-Garcia E, Stanley BH, Sublette ME, Mann JJ. Toward a biosignature for suicide. Am J Psychiatry. 2014; 171:1259–1277. [PubMed: 25263730]

Pantazopoulos H, Lange N, Baldessarini RJ, Berretta S. Parvalbumin neurons in the entorhinal cortex of subjects diagnosed with bipolar disorder or schizophrenia. Biol Psychiatry. 2007; 61:640–652. [PubMed: 16950219]

Pelvig DP, Pakkenberg H, Stark AK, Pakkenberg B. Neocortical glial cell numbers in human brains. Neurobiol Aging. 2008; 29:1754–1762. [PubMed: 17544173]

Pierri JN, Volk CL, Auh S, Sampson A, Lewis DA. Somal size of prefrontal cortical pyramidal neurons in schizophrenia: differential effects across neuronal subpopulations. Biol Psych. 2003; 54:111–120.

Rajkowska G, Miguel-Hidalgo JJ, Dubey P, Stockmeier CA, Krishnan KR. Prominent reduction in pyramidal neurons density in the orbitofrontal cortex of elderly depressed patients. Biol Psychiatry. 2005; 58:297–306. [PubMed: 15953590]

Rajkowska G, Miguel-Hidalgo JJ, Makkos Z, Meltzer H, Overholser J, Stockmeier C. Layer-specific reductions in GFAP-reactive astroglia in the dorsolateral prefrontal cortex in schizophrenia. Schizophr Res. 2002; 57:127–138. [PubMed: 12223243]

Rajkowska G, Miguel-Hidalgo JJ, Wei J, Dilley G, Pittman SD, Meltzer HY, Overholser JC, Roth BL, Stockmeier CA. Morphometric evidence for neuronal and glial prefrontal cell pathology in major depression. Biol Psych. 1999; 45:1085–1098.

Rajkowska G, O'Dwyer G, Teleki Z, Stockmeier CA, Miguel-Hidalgo JJ. GABAergic neurons immunoreactive for calcium binding proteins are reduced in the prefrontal cortex in major depression. Neuropsychopharmacology. 2007; 32:471–482. [PubMed: 17063153]

Rajkowska G, Stockmeier CA. Astrocyte pathology in major depressive disorder: insights from human postmortem brain tissue. Curr Drug Targets. 2013

Reynolds GP, Zhang ZJ, Beasley CL. Neurochemical correlates of cortical GABAergic deficits in schizophrenia: selective losses of calcium binding protein immunoreactivity. Brain Res Bull. 2001; 55:579–584. [PubMed: 11576754]

Roy A, Dejong J, Ferraro T. CSF GABA in depressed patients and normal controls. Psychol Med. 1991; 21:613–618. [PubMed: 1719577]

Sanacora G, Gueorguieva R, Epperson CN, Wu YT, Appel M, Rothman DL, Krystal JH, Mason GF. Subtype-specific alterations of gamma-aminobutyric acid and glutamate in patients with major depression. Arch Gen Psychiatry. 2004; 61:705–713. [PubMed: 15237082]

Sanacora G, Mason GF, Rothman DL, Krystal JH. Increased occipital cortex GABA concentrations in depressed patients after therapy with selective serotonin reuptake inhibitors. Am J Psychiatry. 2002; 159:663–665. [PubMed: 11925309]

Sanacora G, Saricicek A. GABAergic contributions to the pathophysiology of depression and the mechanism of antidepressant action. CNS Neurol Disord Drug Targets. 2007; 6:127–140. [PubMed: 17430150]

Schwenzer M, Zattarin E, Grozinger M, Mathiak K. Impaired pitch identification as a potential marker for depression. BMC Psychiatry. 2012; 12:32. [PubMed: 22515473]

Selemon LD, Mrzljak J, Kleinman JE, Herman MM, Goldman-Rakic PS. Regional specificity in the neuropathologic substrates of schizophrenia: a morphometric analysis of Broca's area 44 and area 9. Arch Gen Psych. 2003; 60:69–77.

Sequeira A, Klempan T, Canetti L, ffrench-Mullen J, Benkelfat C, Rouleau GA, Turecki G. Patterns of gene expression in the limbic system of suicides with and without major depression. Mol Psychiatry. 2007; 12:640–655. [PubMed: 17353912]

Sequeira A, Mamdani F, Ernst C, Vawter MP, Bunney WE, Lebel V, Rehal S, Klempan T, Gratton A, Benkelfat C, Rouleau GA, Mechawar N, Turecki G. Global brain gene expression analysis links glutamatergic and GABAergic alterations to suicide and major depression. PLoS One. 2009; 4:e6585. [PubMed: 19668376]

Sequeira A, Morgan L, Walsh DM, Cartagena PM, Choudary P, Li J, Schatzberg AF, Watson SJ, Akil H, Myers RM, Jones EG, Bunney WE, Vawter MP. Gene expression changes in the prefrontal cortex, anterior cingulate cortex and nucleus accumbens of mood disorders subjects that committed suicide. PLoS One. 2012; 7:e35367. [PubMed: 22558144]

Shah PJ, Glabus MF, Goodwin GM, Ebmeier KP. Chronic, treatment-resistant depression and right fronto-striatal atrophy. Br J Psychiatry. 2002; 180:434–440. [PubMed: 11983641]

Shelton RC, Claiborne J, Sidoryk-Wegrzynowicz M, Reddy R, Aschner M, Lewis DA, Mirnics K. Altered expression of genes involved in inflammation and apoptosis in frontal cortex in major depression. Mol Psychiatry. 2011; 16:751–762. [PubMed: 20479761]

Shenton ME, Dickey CC, Frumin M, McCarley RW. A review of MRI findings in schizophrenia. Schizophrenia Research. 2001; 49:1–52. [PubMed: 11343862]

Sibille E, Morris HM, Kota RS, Lewis DA. GABA-related transcripts in the dorsolateral prefrontal cortex in mood disorders. Int J Neuropsychopharmacol. 2011; 14:721–734. [PubMed: 21226980]

Skilbeck KJ, Johnston GA, Hinton T. Stress and GABA receptors. J Neurochem. 2010; 112:1115–1130. [PubMed: 20002524]

Smiley JF, Bleiwas C. Embedding matrix for simultaneous processing of multiple histological samples. J Neurosci Methods. 2012; 209:195–198. [PubMed: 22710286]

Smiley JF, Hackett TA, Bleiwas C, Mann JJ, Rosoklija G, Dwork AJ. Reduced neuron density in primary auditory cortex of subjects with major depression. Biol Psychiatry. 2014; 75:181S.

Smiley JF, Hackett TA, Preuss TM, Bleiwas C, Figarsky K, Mann JJ, Rosoklija G, Javitt DC, Dwork AJ. Hemispheric asymmetry of primary auditory cortex and Heschl's gyrus in schizophrenia and nonpsychiatric brains. Psychiatry Res. 2013

Smiley JF, Konnova K, Bleiwas C. Cortical thickness, neuron density and size in the inferior parietal lobe in schizophrenia. Schizophrenia Research. 2012; 136:43–50. [PubMed: 22304984]

Smiley JF, Rosoklija G, Mancevski B, Mann JJ, Dwork AJ, Javitt DC. Altered volume and hemispheric asymmetry of the superficial cortical layers in the schizophrenia planum temporale. Eur J Neurosci. 2009; 30:449–463. [PubMed: 19656176]

Smiley JF, Rosoklija G, Mancevski B, Pergolizzi D, Figarsky K, Bleiwas C, Javitt DC, Dwork AJ. Hemispheric comparisons of neuron density in the planum temporale of schizophrenia and nonpsychiatric brains. Psychiatric Research: Neuroimaging. 2011; 192:1–11. [PubMed: 21377842]

Smiley JF, Saito M, Bleiwas C, Masiello K, Ardekani B, Guilfoyle DN, Gerum S, Wilson DA, Vadasz C. Selective reduction of cerebral cortex GABA neurons in a late gestation model of fetal alcohol spectrum disorder. Alcohol. 2015; 49:571–580. [PubMed: 26252988]

Stark AK, Sanz-Arigita E, Pakkenberg B. Glial cell loss in the anterior cingulate cortex, a subregion of the prefrontal cortex, in subjects with schizophrenia. Am J Psychiatry. 2004; 161:882–888. [PubMed: 15121654]

Stockmeier CA, Mahajan GJ, Konick LC, Overholser JC, Jurjus GJ, Meltzer HY, Uylings HB, Friedman L, Rajkowska G. Cellular changes in the postmortem hippocampus in major depression. Biol Psychiatry. 2004; 56:640–650. [PubMed: 15522247]

Sweet RA, Bergen SE, Sun Z, Sampson AR, Pierri JN, Lewis DA. Pyramidal cell size reduction in schizophrenia: evidence for involvement of auditory feedforward circuits. Biol Psychiatry. 2004; 55:1128–1137. [PubMed: 15184031]

Sweet RA, Dorph-Petersen KA, Lewis DA. Mapping auditory core, lateral belt, and parabelt cortices in the human superior temporal gyrus. J Comp Neurol. 2005; 491:270–289. [PubMed: 16134138]

Takei Y, Kumano S, Hattori S, Uehara T, Kawakubo Y, Kasai K, Fukuda M, Mikuni M. Preattentive dysfunction in major depression: a magnetoencephalography study using auditory mismatch negativity. Psychophysiology. 2009; 46:52–61. [PubMed: 19055502]

Tollkotter M, Pfleiderer B, Soros P, Michael N. Effects of antidepressive therapy on auditory processing in severely depressed patients: a combined MRS and MEG study. J Psychiatr Res. 2006; 40:293–306. [PubMed: 16288924]

Torrey EF. Schizophrenia and the inferior parietal lobule. Schiz Res. 2007; 97:215–225.

Tripp A, Oh H, Guilloux JP, Martinowich K, Lewis DA, Sibille E. Brain-derived neurotrophic factor signaling and subgenual anterior cingulate cortex dysfunction in major depressive disorder. Am J Psychiatry. 2012; 169:1194–1202. [PubMed: 23128924]

Underwood MD, Kassir SA, Bakalian MJ, Galfalvy H, Mann JJ, Arango V. Neuron density and serotonin receptor binding in prefrontal cortex in suicide. Int J Neuropsychopharmacol. 2012; 15:435–447. [PubMed: 21733245]

Uranova NA, Vostrikov VM, Orlovskaya DD, Rachmanova VI. Oligodendroglial density in the prefrontal cortex in schizophrenia and mood disorders: a study from the Stanley Neuropathology Consortium. Schizophr Res. 2004; 67:269–275. [PubMed: 14984887]

Volk DW, Matsubara T, Li S, Sengupta EJ, Georgiev D, Minabe Y, Sampson A, Hashimoto T, Lewis DA. Deficits in transcriptional regulators of cortical parvalbumin neurons in schizophrenia. Am J Psychiatry. 2012; 169:1082–1091. [PubMed: 22983435]

von Economo, C. The cytoarchitectonics of the human cerebral cortex. Oxford University Press; London: 1929.

Wallace MN, Johnston PW, Palmer AR. Histochemical identification of cortical areas in the auditory region of the human brain. Exp Brain Res. 2002; 143:499–508. [PubMed: 11914796]

Wang AY, Lohmann KM, Yang CK, Zimmerman EI, Pantazopoulos H, Herring N, Berretta S, Heckers S, Konradi C. Bipolar disorder type 1 and schizophrenia are accompanied by decreased density of parvalbumin- and somatostatin-positive interneurons in the parahippocampal region. Acta Neuropathol. 2011; 122:615–626. [PubMed: 21968533]

West MJ, Gundersen HJG. Unbiased stereological estimation of the number of neurons in the human hippocampus. J Comp Neurol. 1990; 296:1–22. [PubMed: 2358525]

Woo TU, Miller JL, Lewis DA. Schizophrenia and the parvalbumin-containing class of cortical local circuit neurons. Am J Psychiatry. 1997; 154:1013–1015. [PubMed: 9210755]

Zhang ZJ, Reynolds GP. A selective decrease in the relative density of parvalbumin-immunoreactive neurons in the hippocampus in schizophrenia. Schizophr Res. 2002; 55:1–10. [PubMed: 11955958]

Zwanzger P, Zavorotnyy M, Diemer J, Ruland T, Domschke K, Christ M, Michael N, Pfleiderer B. Auditory processing in remitted major depression: a long-term follow-up investigation using 3T-fMRI. J Neural Transm. 2012; 119:1565–1573. [PubMed: 22926663]

Research Highlights

- Auditory cortex was evaluated in major depression and schizophrenia
- Lower GABA neuron density was found in major depression subjects
- Lower density was significant in calbindin and calretinin interneuron subtypes
- Comparable changes were not found in total neuron or glia cell populations
- The findings indicate wide-spread cortical GABA changes in major depression

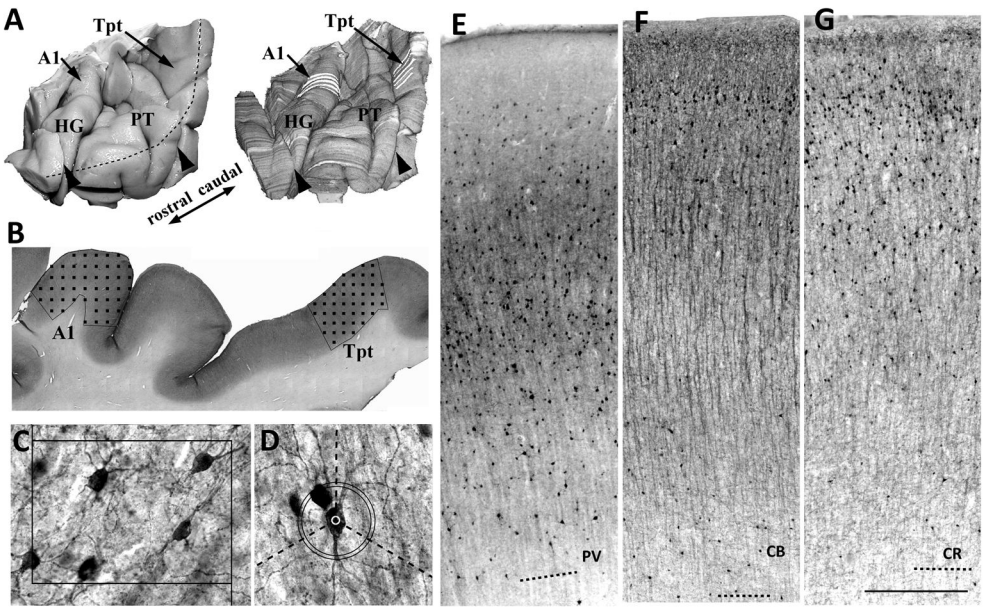

Figure 1.

A) 3-d reconstructions (right) were made from block-face images taken during sectioning. Cellular measurements in areas A1 and Tpt were sample at 4–6 evenly spaced sections (white lines) in each area. Black arrowheads show where tissue was blocked into consecutive pieces at autopsy. The black segmented line shows the crest of the superior temporal gyrus. HG, Heshcl's gyrus. Pt, planum temporal. **B)** In each area, the cortex was sampled with a grid of optical disector sampling sites (black squares). **C)** Cell densities were sampled with optical disector counting boxes, drawn on image z-stacks of taken at each sampling site. Box width = 110 microns. **D)** Cell size and cell labeling density were sampled from cells counted with the optical disectors. Cell size was the average length of 3 radii from the cell center to its soma edge, that was measured along 3 isotropic lines from the cell center (dashed lines). Cell labeling density was the difference between mean foreground density at the cell center (white circle) and the modal background density measured at a band 55–60 microns from the cell center (black circles). **E–G)** Examples are shown of PV **(E)**, CB **(F)**and CR **(G)** labeling in area Tpt. The quality of immunolabeling was very good in this tissue that was fixed only 5 days in phosphate buffered formalin. Dashed lines = white matter borders. Scale bar in G = 500 microns.

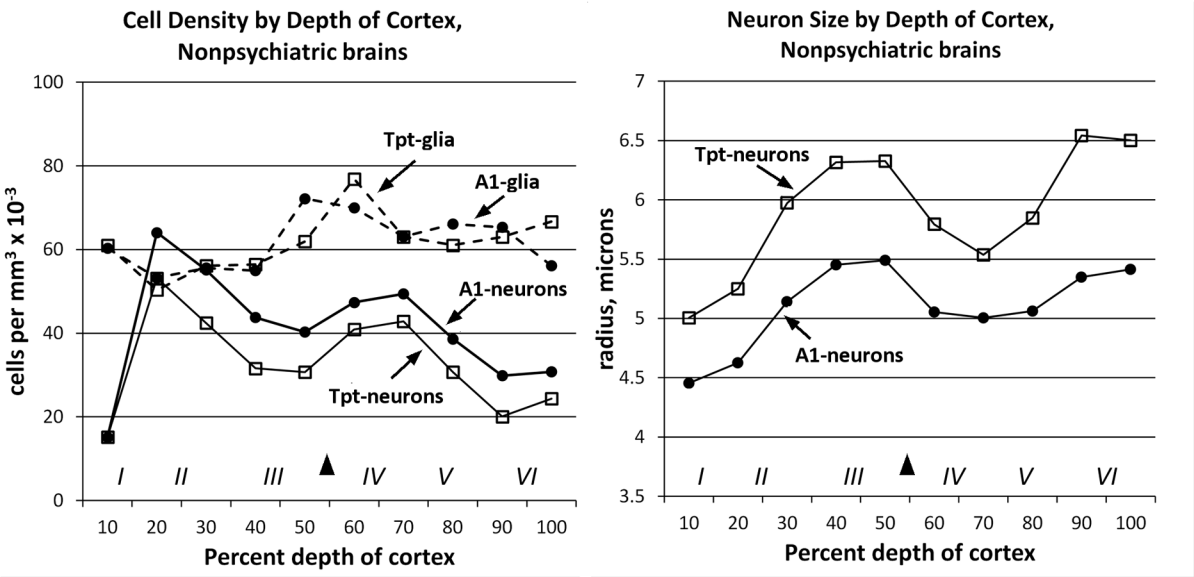

Figure 2.

Total neuron and glia densities and sizes from non-psychiatric brains are graphed by percent depth of cortex. In each graph the black arrowhead shows the location of the top of layer IV, and the Roman numerals show the approximate location of cortical layers. **A)** Cell density measurements showed that area A1 (filled symbols) had higher neuron density than area Tpt (open symbols) across the depth of cortex. Glia densities (dashed lines) were similar in A1 and Tpt. **B)** Neuron size measurements showed that area A1 had smaller neurons in all layers compared to area Tpt. Glia sizes were not measured.

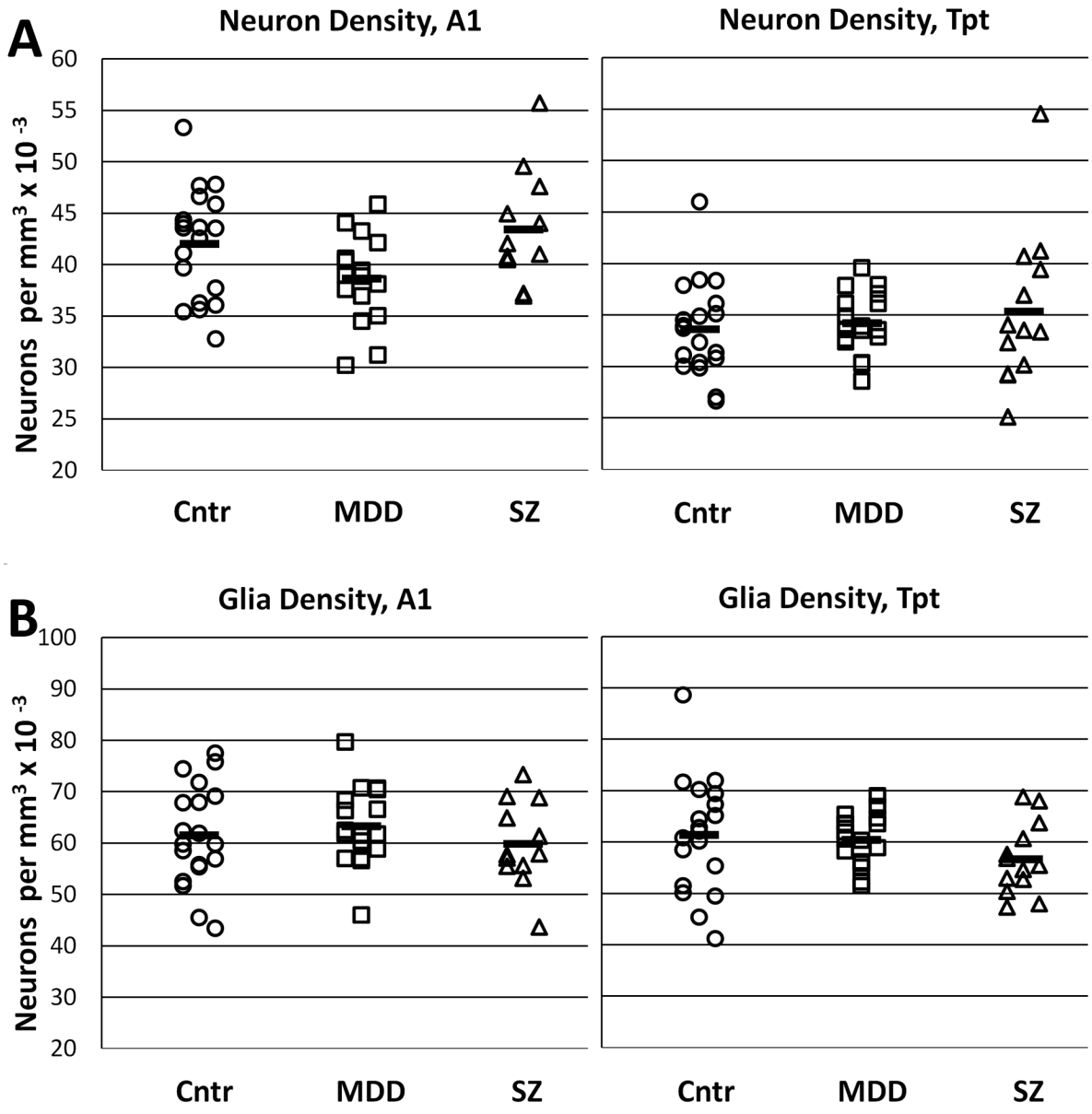

Figure 3.

Graphs show total neuron and glia densities in areas A1 and Tpt. **A)** Neuron densities were slightly lower in area A1 in MDD subjects, but this difference was not evident in area Tpt, and was not statistically significant. **B)** Glial densities were similar in both areas and in all three diagnostic groups. Cntr = non-psychiatric control group.

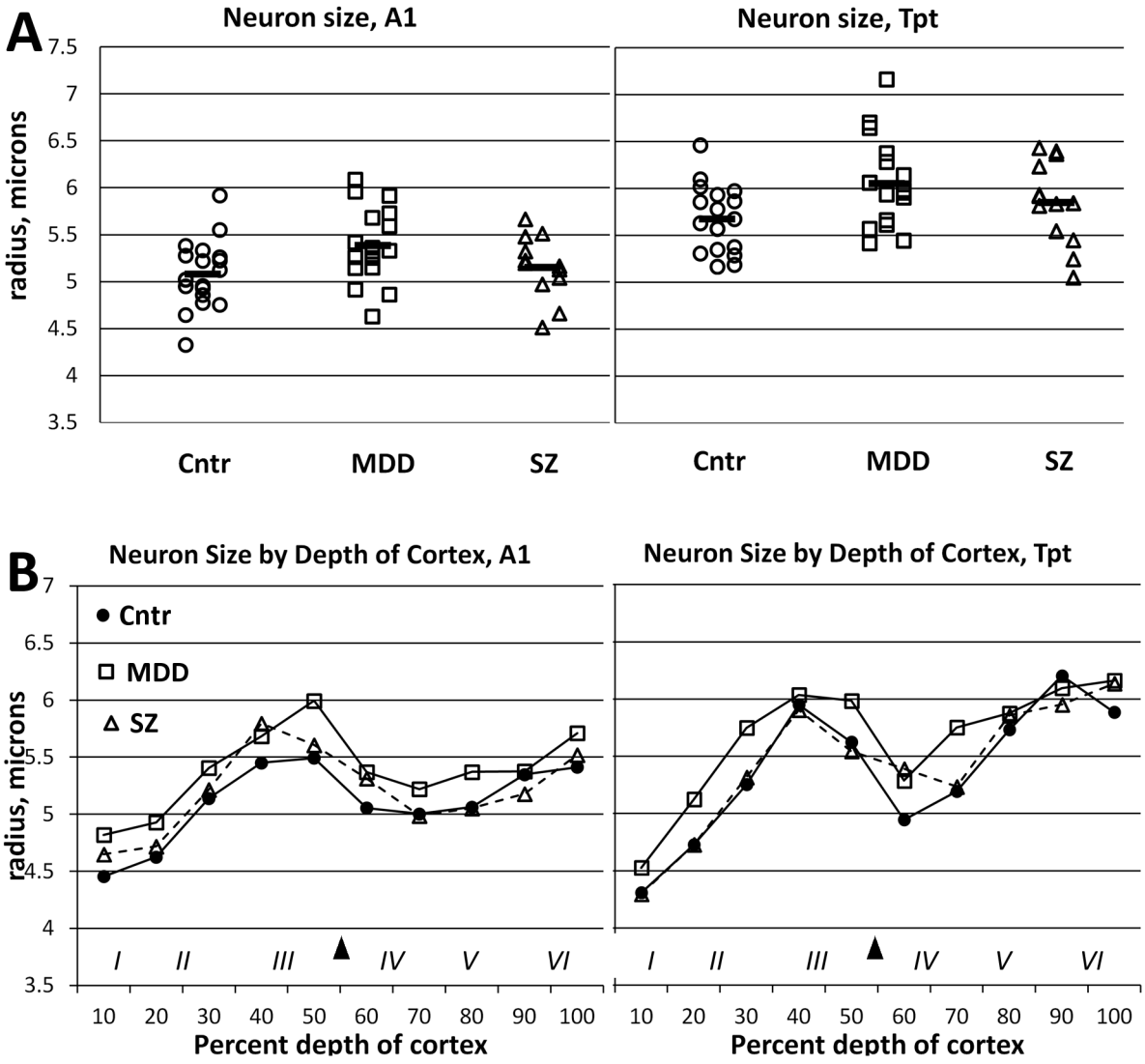

Figure 4.

A) Neuron size was about 6% greater in MDD compared to non-psychiatric controls, in both areas A1 and Tpt. The overall group difference was statistically significant ($p = 0.02$) in the primary statistical model, but not ($p = 0.12$) in a secondary model that included pH as a covariate; see Results section 3.1. **B)** Separation of neuron size measurements by depth of cortex indicated that larger neuron size in MDD was present in both upper and lower cortical layers. Cntr = non-psychiatric control group.

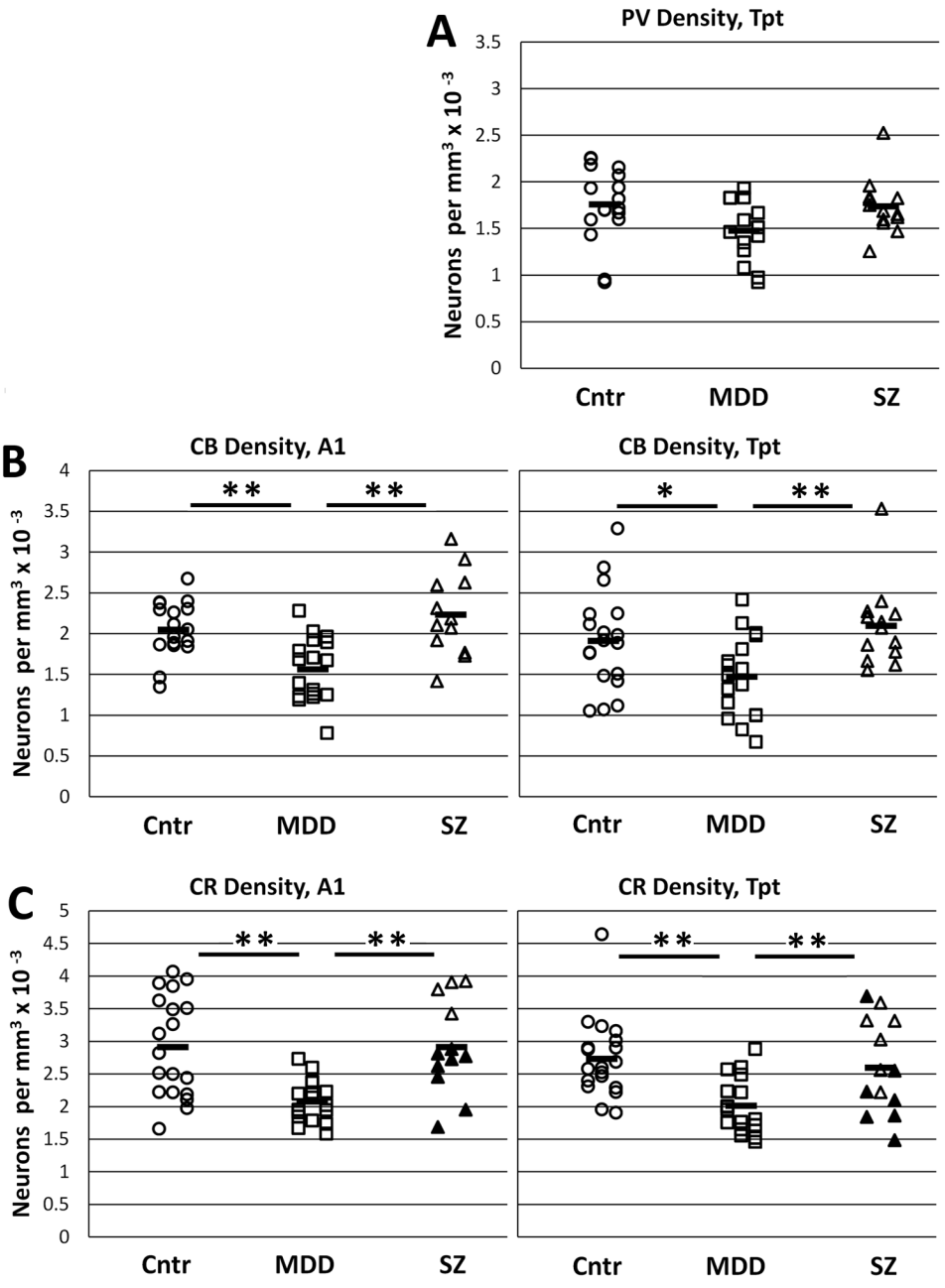

Figure 5.

Graphs show densities of interneuron subtypes that were measured in A1 (left) or Tpt (right). **A)** PV cell density, measured only in area TPt was about 16% lower density in MDD subjects compared to the other groups, but the difference was not statistically significant. **B)** CB density in MDD was significantly reduced in both areas A1 and Tpt. **C)** CR density in MDD was significantly reduced in both areas A1 and Tpt. In the SZ group, the subjects who died by suicide (filled triangles) had comparatively lower densities in both areas A1 and Tpt. (* $p < 0.05$, **$p < 0.01$, t-tests).

J Chem Neuroanat. Author manuscript; available in PMC 2017 October 01.

Table 1

Description of brain samples.

Variable	Cntr (N=20)	MDD (N=17)	SZ (N=14)	p values* MDD-Cntr	p values* SZ-Cntr
Demographic					
Age at death (years)	49.5 (15.5)**	52.5 (14.5)	51.2 (17.7)	0.69	0.90
Brain weight (grams)	1,440 (145)	1,373 (105)	1,331 (202)	0.24	0.11
Gender (male:female)	14:6	9:8	7:7	0.51	0.48
Race	- All caucasian, of Macedonian or Albanian descent -				
Histological					
Postmortem interval (hours)	15.9 (6.9)	14.1 (8.8)	12.4 (5.3)	0.47	0.10
Storage time (months)	26 (14)	33 (11)	20 (12)	0.14	0.16
pH***	6.44 (0.32)	6.37 (0.26)	6.33 (0.29)	0.46	0.37
Clinical					
Cause of Death					
Suicide	0	17	8		
Suicide by poison	0	5	0		
Homicide or violent accident	12	0	0		
Myocardial infarct/ heart failure	5	0	4		
Other	3	0	2		
Major depression, severe and/or recurrent		12			
Major depression, with psychosis		6			
SRI exposure		4	1		
Tricyclic antidepressant exposure		8	4		
Schizophrenia subtype (undifferentiated: paranoid: schizophreniform: schizoaffective)			6:6:1:1		
Lifetime antipsychotic exposure (< 1 month; 1–10 years; > 10years)		0:1:0	1:5:8		

* p values from t-tests, or chi-square test for gender

** Mean (S.D.)

*** pH values missing from 4 SZ and 2MDD subjects

Table 2

Summary of cellular measurements.

	Descriptive statistics									Model-based inferences*	
	A1				Tpt						
	N	Ave	**%CV	*** ratio	N	Ave	%CV	ratio	ratio, A1/Tpt	Diagnosis p-val.	Area p-val.
CELL DENSITY											
Total neuron density, per cubic millimeter											
Cntr	19	42,069	15	-	19	34,147	17	-	1.23		
MDD	17	38,362	15	0.91	17	34,608	10	1.01	1.11		
SZ	12	43,333	10	1.03	13	36,831	13	1.08	1.18	0.12	**3.8E-08**
Glia cell density, per cubic millimeter											
Cntr	19	61,381	16	-	19	62,480	20	-	0.98		
MDD	17	62,733	13	1.02	17	61,288	11	0.98	1.02		
SZ	12	59,483	8	0.97	13	59,766	13	0.96	1.00	0.48	0.97
Parvalbumin neuron density, per cubic millimeter											
Cntr	-	-	-	-	17	1,760	23	-	-		
MDD	-	-	-	-	14	1,476	22	0.84	-		
SZ	-	-	-	-	13	1,737	17	0.99	-	0.13	-
Calbindin neuron density, per cubic millimeter											
Cntr	18	2,050	17	-	18	1,912	32	-	1.07		
MDD	17	1,565	25	0.76	17	1,472	34	0.77	1.06		
SZ	12	2,237	23	1.09	13	2,099	24	1.10	1.07	**4.9E-05**	0.12
Calretinin neuron density, per cubic millimeter											
Cntr	19	2,918	26	-	19	2,735	22	-	1.07		
MDD	17	2,081	16	0.71	17	2,013	21	0.74	1.03		
SZ	12	2,915	25	1.00	13	2,600	28	0.95	1.12	**1.1E-05**	0.06
CELL SIZE											
Total neuron size, radius in microns											
Cntr	19	5.09	7	-	18	5.67	6	-	0.90		
MDD	17	5.39	7	1.06	17	6.05	8	1.07	0.89		
SZ	12	5.16	6	1.01	13	5.85	8	1.03	0.88	**0.02**	**2.7E-14**

	Descriptive statistics									Model-based inferences*		
	A1				Tpt							
	N	Ave	**%CV	*** ratio	N	Ave	%CV	ratio	ratio, A1/Tpt		Diagnosis p-val.	Area p-val.
Parvalbumin neuron size, radius in microns												
Cntr	-	-	-	-	17	6.65	11	-	-			
MDD	-	-	-	-	14	6.89	6	1.04	-			
SZ	-	-	-	-	13	6.85	7	1.03	-		0.34	-
Calbindin neuron size, radius in microns												
Cntr	18	5.77	7	-	18	6.11	8	-	0.94			
MDD	17	6.11	6	1.06	17	6.48	7	1.06	0.94			
SZ	12	5.86	6	1.02	13	6.03	6	0.99	0.97		**0.03**	**2.0E-06**
Calretinin neuron size, radius in microns												
Cntr	19	4.81	6	-	19	5.13	5	-	0.94			
MDD	17	4.80	7	1.00	17	5.03	4	0.98	0.95			
SZ	12	4.79	6	1.00	13	4.96	4	0.97	0.97		0.27	**3.1E-09**
CELL IMMUNOLABELING DENSITY												
Parvalbumin neuron labeling density												
Cntr	-	-	-	-	17	60.8	12	-	-			
MDD	-	-	-	-	14	61.9	21	1.02	-			
SZ	-	-	-	-	13	62.5	15	1.03	-		0.76	-
Calbindin neuron labeling density												
Cntr	18	68.7	13	-	18	67.2	14	-	1.02			
MDD	17	62.1	18	0.90	17	71.8	14	1.07	0.87			
SZ	12	67.9	12	0.99	13	73.2	13	1.09	0.93		0.11	0.03
Calretinin neuron labeling density ****												
Cntr	19	60.5	25	-	19	65.2	22	-	0.93			
MDD	17	53.1	21	0.88	17	47.2	30	0.72	1.12	**A1**	0.08	
SZ	12	54.5	38	0.90	13	62.3	23	0.96	0.87	**Tpt**	**4.0E-04**	0.79

* Outcomes measured at 2 brain areas were modeled using mixed effects models with main effects for diagnosis and area, adjusting for age, sex, pmi and storage time. See Methods section 2.9.

** %CV = 100 x Standard Deviation/Mean.

*** ratio = (MDD or SZ)/non-psychiatric control.

**** The model for Calretinin neuron labeling density has a significant diagnosis-by-area interaction and areas were evaluated separately. See Results section 3.4.

Table 3

Cortex thickness *

	Cntr	SZ	MDD	p-value SZ-Cntr	p-value MDD-Cntr
HG	2.65 (0.24)	2.53 (0.23)	2.59 (0.23)	0.19	0.48
A1	2.73 (0.42)	2.51 (0.24)	2.64 (0.32)	0.13	0.51
PT total	2.69 (0.28)	2.66 (0.23)	2.68 (0.17)	0.75	0.93
PT rostral	2.79 (0.23)	2.79 (0.22)	2.80 (0.18)	0.93	0.83
PT caudal	2.56 (0.33)	2.59 (0.25)	2.54 (0.19)	0.79	0.87
Tpt	2.82 (0.33)	2.77 (0.33)	2.85 (0.33)	0.7	0.96

* Thickness in millimeters (Standard deviation)